Creation of Ultra-Low Friction and Wear Surfaces for Micro-Devices Using Carbon Films

J. J. Rha[1], S. C. Kwon[1], J. R. Cho[1], W. Yim Shon[2], and N. Saka[2]

[1]*Korea Institute of Machinery and Materials, Surface Engineering Department, Korea*

[2]*Massachussetts Institute of Technology, Department of Mechanical Engineering, USA*

Abstract

Certain micro-devices require sliding contact between components; micro-engines, micro-motors, micro-gears, and near-contact or contact recording hard disk drives are some examples. In these devices tribological problems--namely friction, wear and stiction—determine device efficiency and lifetime. Newly developed carbon films show ultra low friction (lower than 0.05), low wear coefficient (lower than 10^{-8}), and high contact angle of water (higher than 85 degrees). This film has very low adherent property that results in ultra low friction and high contact angle. The hardness and elastic modulus are lower than H-DLC but the ratio of hardness to modulus is similar to values for H-DLC that results in low wear rate. Even though these carbon film has low hardness (2 to 10 GPa), it can be used as a protective layer in micro-devices because the

applied load is very light and contact area is large in micro-device applications. A new oscillating compliant beam method was used to measure friction and wear.

Keywords: low friction, wear, contact angle, carbon film, elastic contact, and adhesion.

1. Introduction

Microsystems, such as micro-electromechanical systems (MEMS) and magnetic recording systems, have extremely low tolerance for friction and wear since even the smallest wear particles could cause seizure and catastrophic failure, but liquid lubrication is not generally a viable option due to problems associated with stiction and contamination. MEMS components, in particular, are typically only a few microns thick and structurally unable to withstand high surface traction, which presents a problem since surface forces become increasingly dominant as the physical dimensions become smaller [1].

The characteristic length scales (i.e., component size, contact diameter, and so on) of micromechanical systems are typically of the order of microns. Accordingly, it may be more appropriate to treat the tribological issues in Microsystems at the nano- and atomic scale [2] rather than the macroscale [3,4]. It may be reasoned that sliding of components in Microsystems occurs without much wear and deformation, which means that friction depends mostly on the local interatomic forces at the sliding interface.

Tribological properties require low friction, wear, and stiction simultaneously in microsystems. At present, the main obstacle to the development of ultra-low friction systems is the lack of fundamental understanding of the mechanisms of friction in the

regime of sliding without severe deformation and wear, where friction is determined by the atomic interactions between the clean-shearing surfaces. On the other hand stiction problems are solved by using self-assembled monolayers and F-DLC [5-8]. However, these films cannot serve as tribological passivation layer for micro-devices due to wear out easily.

In this study, we would like to verify Shon's claim [9] that the strength of interatomic interaction between the surfaces should be reduced for reducing friction. And he showed the results supporting his claim by molecular dynamic simulations. Also, we would like to suggest a candidate film to serve as tribological passivation layer in micro-devices.

2. Experiments

Carbon films are synthesized by DC magnetron sputtering. Chamber is evacuated lower than 1×10^{-6} Torr and then filled to 3mTorr with Ar gas. Graphite target of 3inch diameter is mounted on DC gun. DC power density is 11W/cm^2. Substrate temperature and RF bias are room temperature and non-applied for normal carbon film or 300^{o}C and –200V applied for optimized one respectively. Film thickness is measured at partially screened sample by AFM (DI NanoScope IIIa). Thicknesses of carbon films are 250nm.

To measure coefficient of friction, oscillating cantilever beam tribometer is used. This apparatus is very useful when applying load and coefficient of friction are small. Fig. 1 shows the appearance of this apparatus. Cantilever beam has the length of 150mm, height of 12.6mm, and thickness of 0.3mm. Its material is spring steel that has a Young's modulus of 201.4Gpa. Four strain gauges are attached one end of cantilever beam for full bridge. Load is applied at the other end of beam mounted slider holder. Applied loads can be adjusted by moving counter balancing weight to forward or backward. A disk specimen is put on a balance that indicates directly applying load during test. In testing by this apparatus, specimen is stationary and cantilever beam is oscillating on the specimen in contacting of slider and disk. According to Shon's thesis [9], coefficient of friction can be calculated by eq. (1).

$$\mu \quad \frac{\Delta f}{4nW} \tag{1}$$

Here, Δf is a difference of force amplitude,

n is the number of oscillations between difference of force amplitude,

W is an applied load.

Applied loads are varied from 1mN to 50 mN to measure coefficient of friction. Silicon Nitride ball ($r=1.5mm$) and Rockwell C diamond indenter ($r=0.2mm$) are used as sliders. Friction tests are conducted five times per specimen and their results are averaged. Sliding distances are varied from 100mm to 500mm depending on applied loads and coefficient of friction because cantilever beam is deviated same amounts for all friction tests. Velocity of slider decreases continuously until stop from 60mm/sec. All friction tests are conducted in ambient air condition with relative humidity of 20 to 40%.

Pull-off forces between silicon nitride AFM tip (VEECO Model OTR8) and disk specimens or diamond coated AFM tip (VEECO Model ULCT-DCBO) and specimens are measured by AFM (DI Model NanoScope IIIa). The spring constants and radii of silicon nitride AFM tip and diamond coated one are 0.56N/m, 20nm, 0.26N/m, and 100nm respectively.

Wear test is conducted by this apparatus as continuous triggering cantilever beam to

attain 1million passes at un-deformed line of cantilever. The surface profile of wear track is measured by optical surface profilometer (SNUPrecision Model SIS2000) after wear test.

Wetting angles of water are measured by sessile drop of water on disk specimens.

3. Results and discussions

3-1. Friction

Fig. 2 shows a typical output of oscillating cantilever beam tribometer. Silicon nitride ball (ϕ=3mm) is used as slider under 1gf-applied load. As shown in fig. 2, Δf and number of oscillations are measured. And then coefficient of friction is calculated as 0.2 by substituting their values to eq. (1).

Likewise this, coefficients of friction are obtained as changing of applied loads between silicon nitride ball and various disk samples such as Si wafer and two carbon films coated on Si wafer. We denote two carbon films as normal and optimized carbon film because optimized carbon film is synthesized specially to have low surface energy. Their results are shown in Fig. 3. Results look like that coefficients of friction are independent on applied loads except for normal carbon film.

It is known that effect of adhesion is large in micro-devices. In order to investigate effect of adhesion in this test, pull-off forces between silicon nitride AFM tip and disk specimens are measured by AFM. Table 1 summarized their results. Pull-off force is directly related to adhesion force of JKR theory [10] as given by eq. (2).

$$F_a \quad \frac{3}{2}\pi\,\gamma\,R \qquad (2)$$

Here, γ is a work of adhesion between AFM tip and a disk specimen

R is a radius of AFM tip.

Work of adhesion is calculated from eq. (2) and summarized in table 2.

In order to verify adhesion effect, apparent Hertz load is calculated by eq. (3) from JKR theory [10]. And summarized in table 3.

$$W_a \quad W + 3\pi r\gamma + \sqrt{6\pi r\gamma W + (3\pi r\gamma)^2} \qquad (3)$$

Here, r is a radius of slider

W is an applied load.

When apparent Hertz loads are calculated, both surfaces of slider and disk specimen are assumed as ideally smooth surfaces. Apparent Hertz loads are quite larger than applied loads as seen table 3. Even though applied loads are changed 50 times, apparent Hertz loads are changed only 5 times for Si wafer. In the case of silicon nitride ball used as slider, adhesion effect cannot be ignored.

Therefore we try to reduce adhesion effect by using diamond indenter as slider, because diamond is known as very low adherent material. Fig. 4 shows coefficients of friction as function of applied loads when Rockwell C diamond indenter is used. In this case, coefficients of friction show clearly the dependence on applied loads and their slopes are very close to ideal slope according to Hertzian behavior. These results imply that status of contact is almost elastic contact.

In order to confirm the adhesion effect of diamond slider, pull-off forces measured between diamond coated AFM tip and specimens are summarized in table 1. Work of adhesion and apparent Hertz load data are calculated and summarized in table 2 and 3 respectively. In this case adhesion effect is very small and apparent Heltz loads are similar to applied loads. Elastic contacting area is larger than plastic contact's. For reducing coefficient of friction in elastic contact, adhesion should be reduced. It is the reason why optimized carbon film shows the smallest coefficient of friction among testing specimens as shown in Fig. 4. If contact occurs with plastic deform, then adhesion property of surface does not affect significantly on coefficient of friction. And Fig. 4 shows that coefficients of friction start to depart from elastic behavior when applied loads are at 100mN and 50mN for normal and optimized carbon films respectively. However, elastic contact will be remained at lower applied load side. Unfortunately, lower load than 1mN cannot be applied with stable contacting in our apparatus. Optimized carbon film has the coefficient of friction lower than 0.02 at applied load of 1mN and 0.01 at 10mN to 50mN.

3-2. Wear

For wear test, 20mN and 50mN load are applied with diamond indenter as slider on

optimized carbon film. And change of coefficient friction is monitored according to number of passes such as Fig. 5. When 20mN load is applied, coefficient of friction is almost unchanged until 2000 passes. After this point, coefficient of friction increases slowly. We cannot observe any wear track after 200,000 passes. To accelerate wear, 50mN load is applied. In this case coefficient of friction increases with number of passes from initial stage. However, coefficient of friction is still lower than 0.05 after 1 million passes.

Fig. 6 is the surface profile of wear track after 1 million passes. The wear depth is lower than 6nm. The wear coefficient of this result is the value of 7.7×10^{-9}. We expect that wear involve the rupture of asperities. When coefficient of wear is calculated, cross-sectional wear area and number of passes are used instead of wear volume and sliding distance in eq. (4).

$$k \quad \frac{V_w H}{L W} \tag{4}$$

Here, V_w is wear volume,

H is hardness of optimized carbon film,

L is sliding distance,

W is applied load.

Fig. 7 shows the results of nanoindentation of normal and optimized carbon film.

Optimized carbon film has low hardness as much as 4.2 GPa at one-tenth of its thickness. Also this film has low elastic modulus of 63 GPa at the same thickness. Although this film has low hardness, its wear coefficient is very low due to the high ratio of hardness to elastic modulus. The ratio of 0.07 is comparable with H-DLC. Further if contact is completely elastic, then sliding can occur without wear.

In this study the effect of surface roughness is not analyzed. However, surface roughness is an important factor to control contacting status. In future work, this effect should be analyzed.

3-3. Contact angle

Contact angle of water is an important parameter to protect failures of micro-devices during drying after wet processing or operating in humid environment. If contacting angle is small, then completing drying is very difficult due to capillary force of water between two adjacent surfaces that should be separated.

Contact angle of water is measured on sessile drop of water on disk, where DI water of 10 μl is dropped. Typical results are 41^o, 64^o, and 85^o for Si, normal, optimized carbon film respectively as shown in Fig. 8.

4. Conclusion

Disk specimens having distinguishable adhesion property such as Si wafer, normal carbon film, and optimized carbon film are tested to investigate friction, wear, and contact angle of water. In friction test, when non-adherent diamond indenter as slider is used, all specimens show almost ideally elastic contacting behavior at their slopes of friction coefficients versus applied loads. And optimized carbon film having the lowest adherent property shows the lowest coefficient of friction as much as lower than 0.05 at applied load ranged 1mN to 50mN. These two facts support clearly that contacts occur elastically in present experiment. In wear test, wear coefficient of optimized carbon film is lower than 10^{-8} with diamond slider. And optimized carbon film has high contact angle as much as 85^{o} that is nearly approaching 90^{o}.

Therefore optimized carbon film seems to be used for a passivation layer of micro-devices because this film satisfies not only low friction and wear but also high contact angle of water simultaneously.

5. References

1. B. Bhushan, Handbook of Micro/Nano Tribology, CRC Press, (1999).
2. B. Bhushan, J. N. Israelachvili, and U, Landman, Nanotribology: Friction, Wear and Lubrication at the Atomic Scale, Nature, 374 (1995) 607-616.
3. E. Rabinowicz, Friction and Wear of Materials, Jhon Wiley & Sons, Inc., New York (1995).
4. N. P. Suh, Tribophysics, Prentice Hall, New Jersey (1986).
5. R. Maboudian, W. Robert Ashurst, and Carlo Carraro, Self-assembled Monolayers as Anti-stiction Coatings for MEMS: Characteristics and Recent Developments, Sensors and Actuators 82 (2000) 219.
6. R. Maboudian and R. T. Howe, Critical Review: Adhesion in Surface Micromechanical Structures, J. Vac. Sci. Technol. B, 15(1) (1997) 1.
7. C. H. Mastrangelo, Adhesion-related Failure Mechanisms in Micromechanical Devices, Tribol. Lett., 3 (1997) 223.
8. Bradley K. Smith, J. J. Sniegowski, and G. LaVigne, Thin Teflon-like Films for Eliminating Adhesion in Released Polysilicon Microstructures, Transducers '97, 1997 International Conference on Solid-State Sensors and Actuators, Chicago, June 16-19 (1997) 245.
9. W. Yim Shon’ thesis, Dynamics of Sliding Mechanisms in Nanosvale Friction, MIT (2002).

10. K. L. Johnson, K. Kendall, A. D. Roberts, Surface Energy and the Contact of Elastic Solids, Proc. R. Soc. Lond. A. 324 (1971) 301-313.

6. Tables

Table 1. Pull-off forces between silicon nitride AFM tip or diamond coated AFM tip and disk specimens are measured by AFM. Silicon nitride AFM tip has the radius of 20nm and the spring constant of 0.56N/m. Diamond coated AFM tip has the radius of 100nm and the spring constant of 0.26N/m.

Kind of AFM tip	Pull-off force (nN)		
	Si	Normal carbon	Optimized carbon
Silicon Nitride	50	33	15
Diamond coated	17.4	10.9	3.9

Table 2. Works of adhesion between AFM tips and disk specimens are calculated by using JKR theory's adhesion force that is equated with pull-off force.

Kind of AFM tip	Work of adhesion (mJ/m^2)		
	Si	Normal DLC	Optimized DLC
Silicon Nitride	530	350	160
Diamond coated	36.9	23.1	8.3

Table 3. Apparent Hertz loads of JKR theory between sliders and disk specimens are calculated by replacing AFM tips with sliders.

Slider	Specimen	Apparent Hertz load [*mN*]					
		Applied load [*mN*]					
		1	2	5	10	20	50
Silicon nitride ball (*r=1.5mm*)	Si	17	19	24	32	42	86
	Normal carbon	12	14	19	26	40	78
	Optimized carbon	6	8	13	19	32	67
Diamond indenter (*r=0.2mm*)	Si	1.45	2.60	5.91	11.25	21.74	52.71
	Normal carbon	1.34	2.46	5.70	10.98	21.36	52.13
	Optimized carbon	1.19	2.27	5.41	10.58	20.81	51.27

7. Figure captions

Figure 1. The appearance of oscillating cantilever beam tribometer.

Figure 2. Typical output signal of oscillating cantilever beam tribometer. And how to measure the difference of force amplitude and number of oscillations are shown.

Figure 3. Plots of friction coefficients versus applied loads in log-log scale with silicon nitride ball slid on Si wafer, normal carbon film, and optimized carbon film.

Figure 4. Plots of friction coefficients versus applied loads in log-log scale with diamond indenter slid on Si wafer, normal carbon film, and optimized carbon film.

Figure 5. Plots of friction coefficients versus number of passes in x-axis of log scale with diamond indenter slid on optimized carbon film at applied loads of 20 and 50 mN.

Figure 6. The Surface profile of wear track in optimized carbon film after 1 million passes.

Figure 7. Harness and elastic modulus of normal and optimized carbon film measured by nanoindentation. Left vertical axis and right one displays values of hardness and elastic modulus, respectively.

Figure 8. Measured contact angle of water on; (a) Si (41^{o}), (b) normal carbon film (64^{o}), and (c) optimized carbon film (85^{o}).

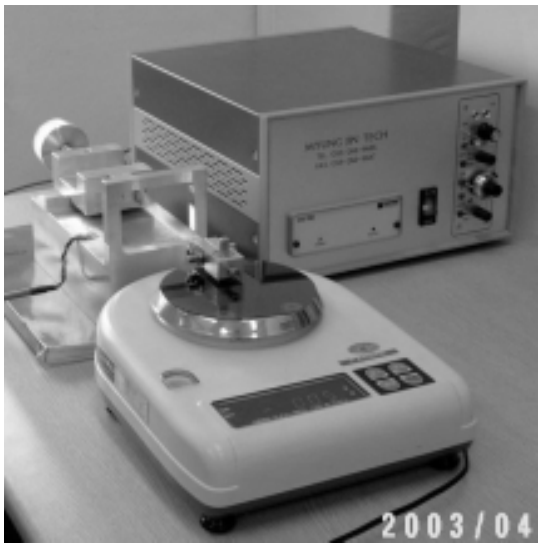

Figure 1.

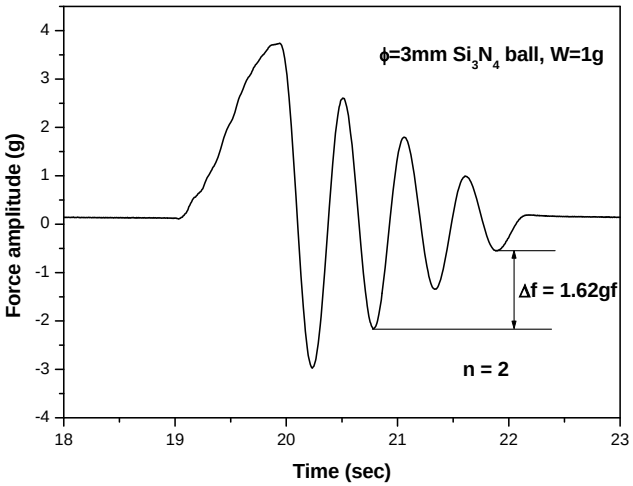
ϕ=3mm Si3N4 ball, W=1g
Δf = 1.62gf
n = 2
Force amplitude (g)
Time (sec)
4
3
2
1
0
-1
-2
-3
-4
18
19
20
21
22
23

Figure 2

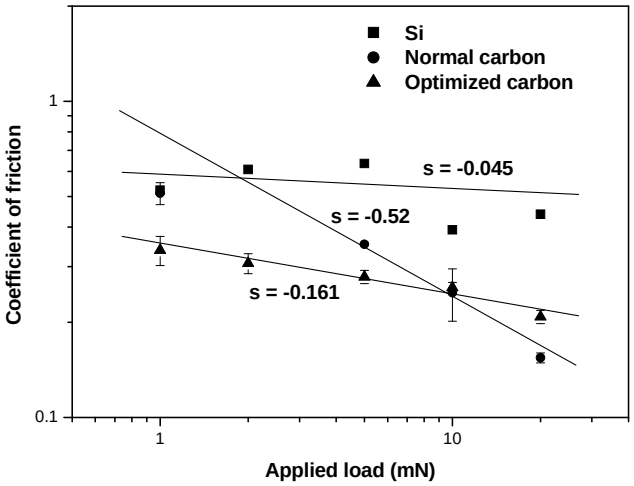
Si
Normal carbon
Optimized carbon
s = -0.045
s = -0.52
s = -0.161
Coefficient of friction
Applied load (mN)
1
0.1
1
10

Figure 3.

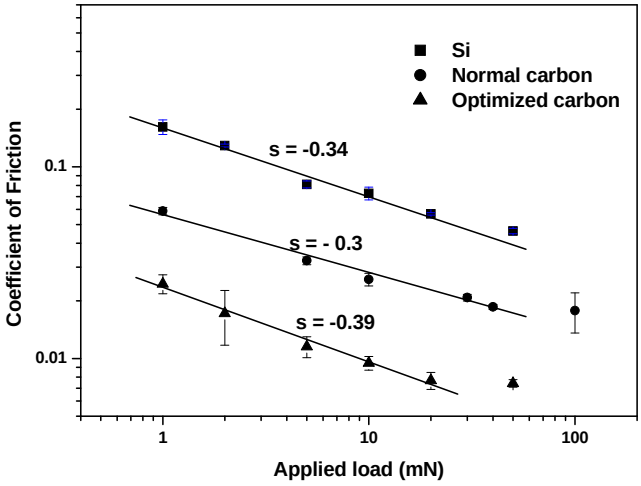
Si
Normal carbon
Optimized carbon
s = -0.34
s = - 0.3
s = -0.39
Coefficient of Friction
0.1
0.01
1
10
100
Applied load (mN)

Figure 4.

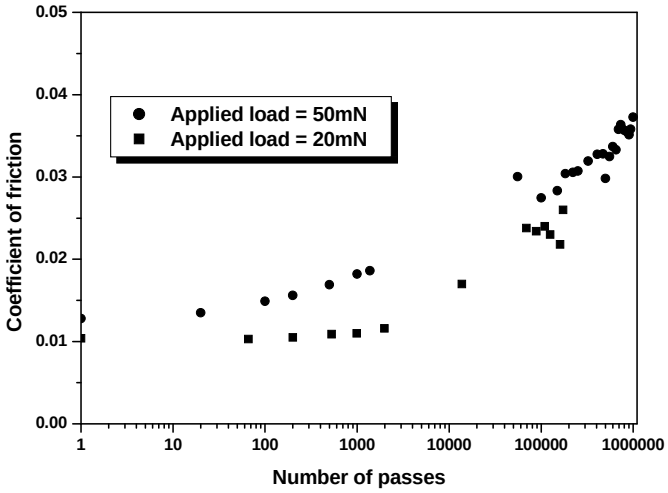
Applied load = 50mN
Applied load = 20mN
Coefficient of friction
Number of passes
0.00
0.01
0.02
0.03
0.04
0.05
1
10
100
1000
10000
100000
1000000

Figure 5.

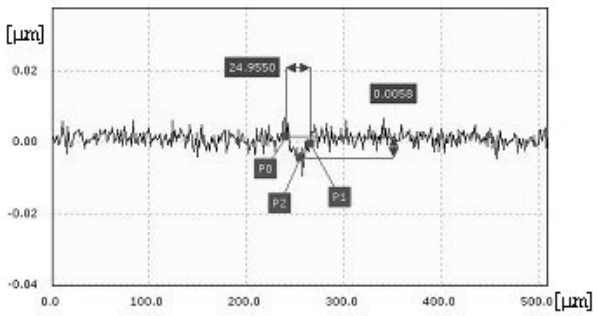
[µm]
0.02
0.00
-0.02
-0.04
24.9550
0.0058
P0
P2
P1
0.0
100.0
200.0
300.0
400.0
500.0
[µm]

Figure 6.

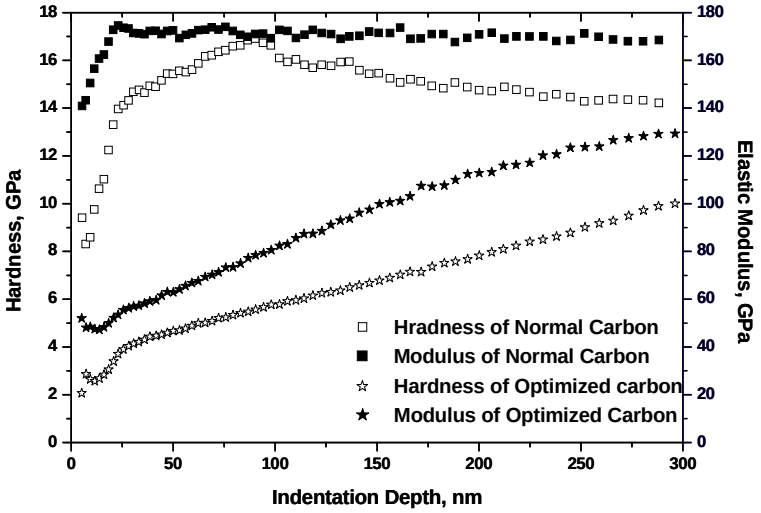
Hardness, GPa
Elastic Modulus, GPa
Indentation Depth, nm
Hradness of Normal Carbon
Modulus of Normal Carbon
Hardness of Optimized carbon
Modulus of Optimized Carbon
0
2
4
6
8
10
12
14
16
18
0
20
40
60
80
100
120
140
160
180
0
50
100
150
200
250
300

Figure 7.

(a)

(b)

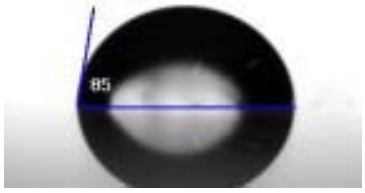

(c)

Figure 8.